Scanning Magnetoresistive Microscopy Study of Quasi-Static Magnetic Switching in Mesoscopic Square Dots: Observation of Field-Driven Transition Between Flux-Closure States

Dipanjan Mazumdar and Gang Xiao

Department of Physics, Brown University, Providence, RI 02912 USA

We used newly developed scanning magnetoresistance microscopy (SMRM) to observe time-lapsed magnetic domain images during magnetic switching in square Permalloy dots. Unlike magnetic force microscopy, the SMRM images measure the *absolute* local magnetic field from any microstructure. SMRM works in an external magnetic field, allowing the measurement of evolution of quasi-static domain structures. We observed a complete magnetic reversal in 5 μm Permalloy dots from a positively saturated state to a negatively saturated state via a mixture of flux-closure states. We also observed field-driven transitions between the various flux closure states at low fields. There appears to be a distribution of switching field and mode, even for geometrically identical dots. This work demonstrates the novel capability of the SMRM technique and the rich switching physics of magnetic square dots.

Index Terms—**Magnetization reversal, magnetoresistive devices, microscopy, Permalloy films.**

I. Introduction

BECAUSE of the rapid development in magnetic data storage and magnetic random access memory [1], [2], a number of magnetic mesoscopic elements such as dots [3], [6]–[8], ellipses [4], [5], and rings [9]–[13] have received much attention in recent years. All these structures have been considered as potential candidates for storage and memory applications. In spite of the promises, there are a number of issues to be resolved. One is the high field needed to switch these magnetic particles. As the lateral size decreases, the switching field becomes higher due to an increasing shape anisotropy. Next, variations in shape, defects, and impurities lead to a distribution of switching field within a batch of magnetic particles fabricated under identical conditions. Furthermore, in small magnetic systems, switching can happen via different intermediary modes, which may also affect the switching field. It is imperative, therefore, to study such distribution to better understand and implement such magnetic small elements.

Various techniques have been employed to study magnetic reversal of patterned systems by imaging domain structures. The popular magnetic force microscopy (MFM) measures the local magnetic field gradient and yields information on domain structures. The lack of absolute field information in this technique can complicate data analysis. MFM also has other limitations, for example, its magnetic tip can strongly disturb the magnetic switching process; and considerable care has to be taken to minimize the effect of the tip, especially while imaging in an external magnetic field [5], [14], [15].

In this work, we used a newly developed scanning magnetoresistance microscope (SMRM) to study the time-lapsed magnetic reversal process in square Permalloy dots under the influence of an external magnetic field. We report the observation of different switching modes and distribution of switching field in an ensemble of squares. Field-driven transitions between the various low-remanence flux closure states are clearly observed. These transitions seem to be a manifestation of the surface roughness and the demagnetization energy term.

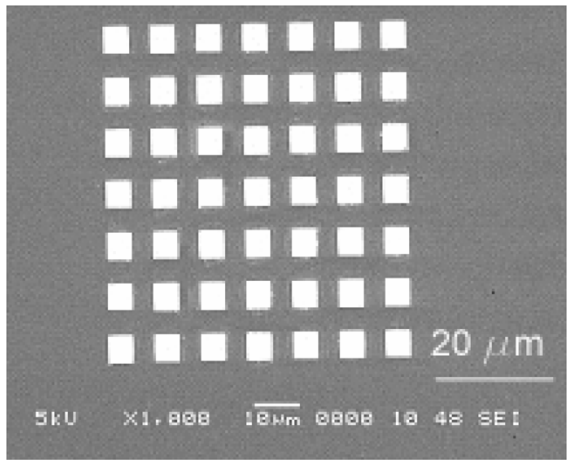

Fig. 1. Scanning electron microscopy image of a 7×7 array of 5 μm Permalloy squares with thickness of 50 nm. The material was prepared using electron-beam evaporation and lithography.

As we will demonstrate, SMRM distinguishes itself in its ability to image absolute magnetic local field, its small probe-sample interference, its long sensor life, and high sensitivity and spatial resolution.

II. Experimental Technique

We fabricated arrays of 5 μm square Permalloy dots for this study. 7×7 arrays of square pattern of e-beam resist were defined on a Si (100) substrate by e-beam lithography at 30 keV beam energy. After development, a polycrystalline trilayer of Ti (5 nm)/$Ni_{80}Fe_{20}$ (50 nm)/Ti (5 nm) was deposited using e-beam evaporation followed by lift-off. Finally, a 150 nm layer of SiO_2

Digital Object Identifier 10.1109/TMAG.2005.851838

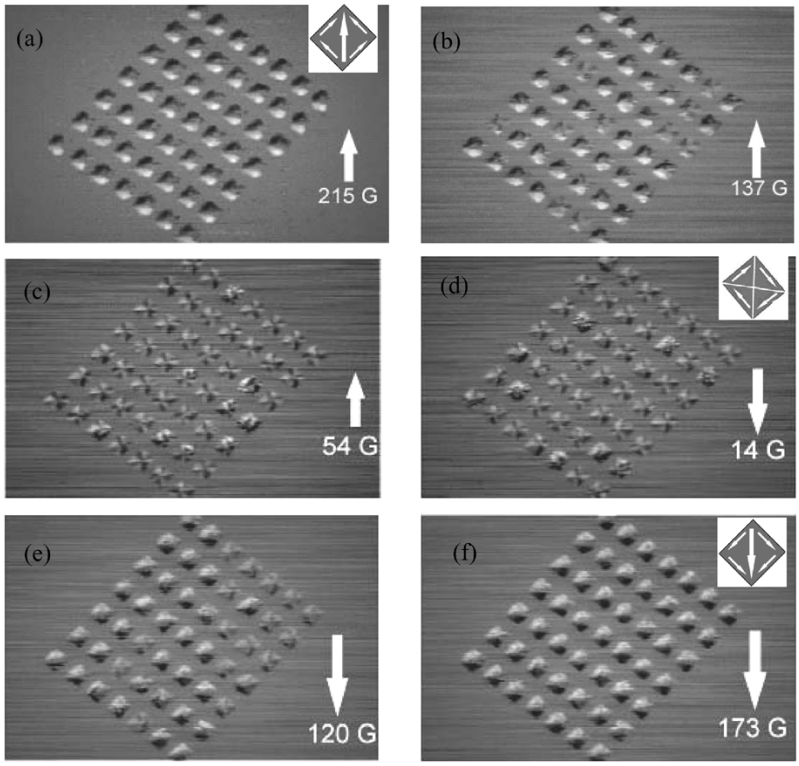

Fig. 2. (a)–(f) SMRM images of the square array under varying external different magnetic field as indicated. The field was applied along the diagonal axis of the squares. Inset in (a), (d), and (f) shows the magnetization configuration in positive saturated, FC, and negative saturated state.

was deposited onto the samples for protection against oxidation and potential damage during raster scanning. Fig. 1 shows an SEM image of a typical array.

To image the magnetic domain structures, we used an SMRM recently developed by our group [16], [17]. The SMRM utilizes a nanoscale magnetoresistive (MR) sensor as a probe to raster scan over the sample surface (X–Y plane). The sensor measures the *absolute* magnetic field along the Z direction. The cross-sectional area of the sensing film determines the active sensing area. For the sensors used in the present study, the sensing region is approximately rectangular with dimensions of 20 nm (determined by thickness) by 100 nm (determined by lithography) [17]. This sets the absolute resolution of the sensor and hence our SMRM. The measured Z field is the average field of this region. Even if the sample scanned has dimensions lower than the sensor area, the sensor responds as if subjected to the average of the field generated by the sample over the entire sensing area.

An X–Y mechanical scanner with 10 nm spatial resolution helps mapping out the magnetic field image in the X–Y plane. The sensor and the protective SiO_2 layer over the magnetic film are in physical contact during raster scanning. While our MR sensor has an ultimate resolution of about 10 nm, the resolution of the microscope is set by roughly the distance between the sensor and sample, which is about 200 nm in our case, mainly due to the protective layer on the sample. The whole setup is computer controlled under a LabVIEW program. The sample is mounted on a rotation stage so that the magnetic structures can be imaged at various angles with respect to the external field. The sensor in the microscope is calibrated by measuring the magnetic field generated by a current carrying wire of known geometry. Hence, the magnetic stray field generated by any magnetic structure can be precisely measured. The microscope is equipped with electromagnets that provide an external field of up to 700 G in the X–Y plane. Since the MR sensor is only sensitive to the Z-component field, external X–Y field that dictates magnetic switching of square dots does not affect the operation of the sensor. This feature gives us the advantage of imaging quasi-static domain structures in varying external fields.

To observe the magnetic reversal process, we programmed the microscope to take a time-lapsed series of magnetic images with each frame corresponding to an external magnetic field, which was decreasing. At the start of the measurement, the field was set at 215 G at 45° from the one edge of the square. This field is large enough to saturate all the magnetic squares along the diagonal axis of the squares. We then reduced the field to a new value, and recorded a corresponding magnetic image, which took about 15 min. We repeated this process again until the field was at −215 G, which negatively saturated all the squares. At the end of the measurement, we organized all the images sequentially and obtained a movie-like presentation of the magnetic reversal process (see [18] for downloading the movie).

III. Results and Discussion

Here, we selectively show some of the images at different fields in Fig. 2. Each image is a magnetic field map of a particular domain structure. The maximum stray field is of the order of 30 G, which depends sensitively on the sensor-sample distance. At the positive field of 215 G [Fig. 2(a)], the strongest fields are located at the two opposite corners of the squares. We will refer to this state as the positively saturated state. This state is similar to the leaf state with the magnetization predominantly along the diagonal. The leaf state has been predicted by micromagnetic simulation [20] in very small Permalloy squares at zero field.

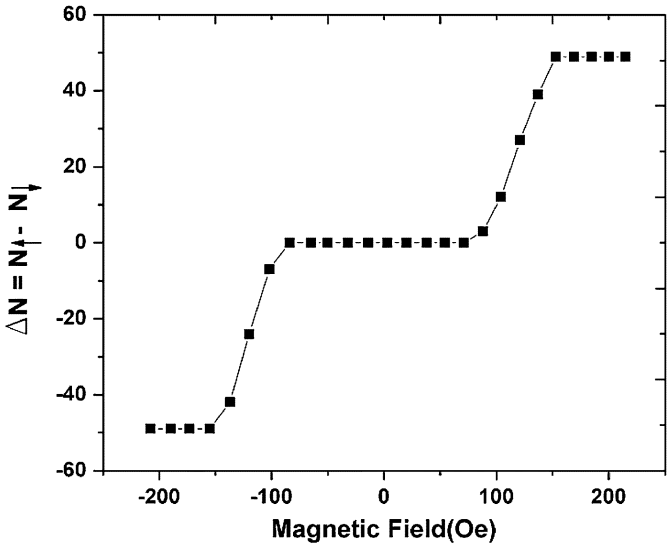

Fig. 3. Difference in the number of positively saturated states and negatively saturated states as a function of external field. The data were extracted from SMRM images as in Fig. 2.

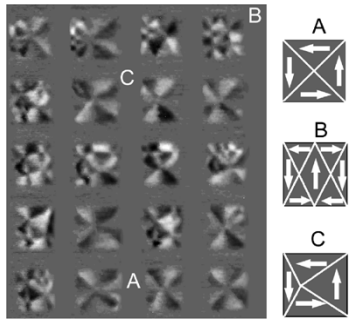

Fig. 4. Closer view of the square dots at remanence. The different intermediate states are seen clearly. Magnetization configurations of a single-vortex FC state (A), diamond state (B), and shifted FC state (C) are shown schematically.

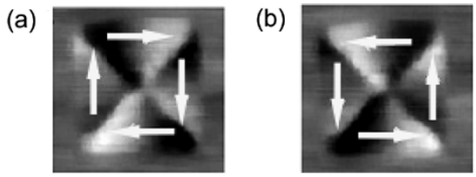

Fig. 5. SMRM images of a single square in a single-vortex state. The CW (a) and CCW (b) magnetization orientation in the two images are distinguished by the opposing dark–bright contrast.

As the field is reduced, nucleation starts to appear in some squares at around 150 G. At 137 G shown in Fig. 2(b), some of the squares change their domain patterns from the saturated state to the flux closure (FC) state. However, at this field, most of the squares still remain in the saturated state. The maximum stray field measured for the FC states is below 5 G. As expected, further decreasing field brings more squares into the FC states [Fig. 2(b)–(d)]. By about 88 G, only two squares remain in the saturated state (not shown in Fig. 2). This observation shows that there is a broad distribution of switching field among these similar squares.

By reversing the magnetic field to about -100 G, reversed or negatively saturated domains start to appear. At -160 G, all the squares are in the negatively saturated states [see Fig. 2(e) and (f)].

To illustrate the magnetization reversal process, we introduce a parameter $\Delta\,\mathrm{N} = \mathrm{N}_{\uparrow} - \mathrm{N}_{\downarrow}$, which is the difference between the number of positively saturated state $(\mathrm{N}_{\uparrow})$ and that of negative saturated state $(\mathrm{N}_{\downarrow})$. In Fig. 3, we plot Δ N as a function of the external field in the same sequence of Fig. 2. Clearly, as the field is changed from 215 to -215 G, the squares undergo the following changes: 1) positively saturated; 2) coexistence of multiple states; 3) flux-closure states; 4) coexistence of multiple states; and 5) negatively saturated. The field distribution for the two transitional states 2) and 4) is nearly 50 G.

The domain structures seen in Fig. 2 are in good agreement with micromagnetic simulations [19]. The magnetization at high fields is parallel to the external magnetic field [see inset in Fig. 2(a)]. This state is comparable to the single domain state. The pinning of the spins at the edges leads to a high stray field as seen in Fig. 2(a) and (f).

A closer look at the low remanence demagnetized states reveals a few more interesting states and physics. Fig. 4 is an SMRM image of 20 squares taken at zero field. Around 40% of the elements are in a single-vortex FC state (A in Fig. 4). Such states are also seen in Fig. 2(b)–(e). Apart from the single-vortex FC state, multivortex states with more complicated domain structures are also seen in the same image. Diamond-like states (B in Fig. 4), showing a double vortex structure with seven or higher domains, and states with slightly shifted vortex core (C in Fig. 4) are among the states seen in the image. All these states have stray field comparable to that of a single-vortex FC state. Such states have been seen before with techniques such as MFM [19]. Our work demonstrates that SMRM not only has similar capability, but also offers new information such as local absolute field that is not sensor (or tip) dependent as in MFM.

An even closer look at a single square in FC state enables us to distinguish between clockwise (CW) and counter-clockwise (CCW) domain configurations. Fig. 5(a) and (b) are remanent SMRM images of a single square in a single-vortex state. The alternating bright–dark contrasts are opposite in the two images implying opposite circulation of spins, as indicated by the arrows.

The most interesting thing we observe in this study is the field-driven transitions between the various flux-closure states. Fig. 6(a)–(d) shows images of the same 20 squares at different fields. Some of the squares, especially in the first two rows, appear to switch from one multidomain state to another and even to the four-domain single-vortex FC state. The rest of the squares appear to be in a stable four-domain FC state. This type of distribution is seen in Fig. 2(c)–(d) also. It is well known from numerical simulations that for mesoscopic squares the demagnetized flux-closure states are the minimum energy states at zero field [20]. So far, simulations and experiments have focused on the minimum energy states at zero field as a function of element size and thickness and shape [21]. The role of the demagnetization energy has so far not been studied. The present work clearly shows that in the mesoscopic regime where demagnetization energy dominates exchange, variations in this term does induce switching between the various low-energy flux closure states.

In the present magnetic structure under study, the only thing that changes with the varying external magnetic field is the demagnetization field on the dots and hence their demagnetization

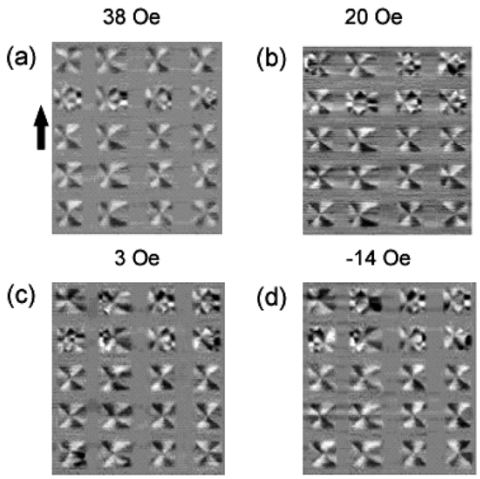

Fig. 6. SMRM images of squares at different fields near zero field. Transitions between various intermediate states are observed. Arrow indicates the positive field direction.

energy. The fact that these flux-closure states appear to switch from one state to another with very little change in external field indicates that the energy barriers separating these different flux-closure states are small. And, as our data reflect, these barriers can be overcome by small changes in the demagnetization energy. From our study, the single-vortex flux-closure state appears to be the minimum energy state. The other states like the Landau state [22], in which four domains are formed, and higher multidomain states are metastable, and changing the field by around 10–15 Oe (due to the combined field of the changing external field and the field generated by the sensor, which is quite low at the sample-sensor distance under study)[1] can trigger transitions between these states. These features have so far never been captured by simulations or by previous experiments. Simulations can provide the global minimum energy states and information on field-driven transitions to other metastable states is almost never predicted. It is important to realize that due to the variation in surface roughness, each element has different demagnetization energy. Hence, even when all identically prepared squares are in an initial saturated state, each has different total energy. This manifests itself in differing switching fields for each element and hence the wide switching field distribution.

IV. Conclusion

We demonstrated that SMRM offers a powerful method of imaging the quasi-static behavior of magnetic domain structures. Mesoscopic Permalloy squares reveal multiple demagnetized states and a very broad switching field distribution despite identical shape and size. We also observed transitions between different flux-closure states.

Acknowledgment

This work was supported by the National Science Foundation under Grant DMR-0306711 and Grant DMR-0080031. The first author would like to thank B. Schrag for technical help and training with SMRM, and X. Liu and W. Shen for their help in sample fabrication.

[1]A clear experimental estimate of the field generated by the sensor is quite difficult owing to the small size of the sensor. But never have we observed significant magnetic changes within the elements under study which has been observed, say, with MFM.

References

[1] S. A. Wolf, D. D. Awschalom, R. A. Buhrman, J. M. Daughton, S. von Molnár, M. L. Roukes, A. Y. Chtchelkanova, and D. M. Treger, "Spintronics: A spin-based electronics vision for the future," *Science*, vol. 294, pp. 1488–1495, 2001.

[2] J. G. Zhu, Y. Zheng, and G. A. Prinz, "Ultrahigh density vertical magnetoresistive random access memory (invited)," *J. Appl. Phys.*, vol. 87, pp. 6668–6673, 2000.

[3] R. P. Cowburn, A. O. Adeyeye, and M. E. Welland, "Configurational anisotropy in nanomagnets," *Phys. Rev. Lett.*, vol. 81, pp. 5414–5417, 1998.

[4] P. Vavassori, O. Donzelli, L. Callegaro, M. Grimsditch, and V. Metluskko, "Magnetic domain structure and magnetic reversal in elliptical dot arrays," *IEEE Trans. Magn.*, vol. 36, no. 5, pp. 2993–2995, Sep. 2000.

[5] X. Zhu, P. Grutter, V. Metlushko, and B. Ilic, "Magnetic force microscopy study of electron beam patterned soft permalloy particles: Techniques and magnetization behavior," *Phys. Rev. B*, vol. 66, pp. 024 423–024 429, 2002.

[6] T. Shinjo, T. Okuno, R. Hassdorf, K. Shigeto, and T. Ono, "Magnetic vortex core observation in circular dots of permalloy," *Science*, vol. 289, pp. 930–932, 2000.

[7] M. Hehn, K. Ounadjela, J.-P. Bucher, F. Rousseaux, D. Decanini, B. Bartenlian, and C. Chappert, "Nanoscale magnetic domains in mesoscopic magnets," *Science*, vol. 272, pp. 1782–1785, 1996.

[8] C. A. F. Vaz, L. Lopez-Diaz, M. Kläui, J. A. C. Bland, T. L. Monchesky, J. Unguris, and Z. Cui, "Direct observation of remanent magnetic states in epitaxial fcc Co small disks," *Phys. Rev. B*, vol. 67, pp. 140 405–140 408, 2003.

[9] Y. G. Yoo, M. Kläui, C. A. F. Vaz, L. J. Heyderman, and J. A. C. Bland, "Switching field phase diagram of Co nanorings magnets," *Appl. Phys. Lett.*, vol. 82, pp. 2470–2472, 2003.

[10] J. Rothman, M. Kläui, L. Lopez-Diaz, C. A. F. Vaz, A. Bleloch, J. A. C. Bland, Z. Cui, and R. Speaks, "Observation of a bi-domain state and nucleation free switching in mesoscopic ring magnets," *Phys. Rev. Lett.*, vol. 86, pp. 1098–1101, 2000.

[11] F. J. Castaño, C. A. Ross, C. Frandsen, A. Eilez, D. Gil, and H. I. Smith, "Metastable states in magnetic nanorings," *Phys. Rev. B*, vol. 67, pp. 184 425–184 429, 2003.

[12] M. Kläui, J. Rothman, L. Lopez-Diaz, C. A. F. Vaz, J. A. C. Bland, and Z. Cui, "Vortex circulation control in mesoscopic ring magnets," *Appl. Phys. Lett.*, vol. 78, pp. 3268–3270, 2001.

[13] S. P. Li, D. Peyrade, M. Natali, A. Lebib, Y. Chen, U. Ebels, L. D. Buda, and K. Ounadjela, "Flux-closure states in cobalt rings," *Phys. Rev. Lett.*, vol. 86, pp. 1102–1105, 2003.

[14] R. D. Gomez, M. C. Shih, R. M. H. New, R. F. W. Pease, and R. L. White, "Switching characteristics of submicron cobalt islands," *J. Appl. Phys.*, vol. 80, no. 1, pp. 342–346, 1996.

[15] X. Zhu, P. Grutter, V. Metlushko, and B. Ilic, "Magnetization reversal and configurational anisotropy of dense permalloy dot arrays," *Appl. Phys. Lett.*, vol. 80, pp. 4789–4791, 2002.

[16] B. D. Schrag and G. Xiao, "Submicron electrical current density imaging of embedded microstructures," *Appl. Phys. Lett.*, vol. 82, pp. 3272–3274, 2003.

[17] B. D. Schrag, "Scanning magnetoresistive microscopy and spintronics based sensing," Ph.D. thesis, Brown University, Providence, RI, 2003.

[18] [Online]. Available: http://physics.brown.edu/physics/userpages/students/Dipanjan_Mazumdar/5m_45deg.mov

[19] G. Gubbiotti, L. Albini, G. Carlotti, M. De Crescenzi, E. Di Fabrizio, A. Gerardino, O. Donzelli, F. Nizzoli, H. Koo, and R. D. Gomez, "Finite size effects in patterned magnetic permalloy films," *J. Appl. Phys.*, vol. 87, no. 9, pp. 5633–5635, 2000.

[20] R. P. Cowburn and M. E. Welland, "Phase transitions in planar magnetic nanostructures," *Appl. Phys. Lett.*, vol. 72, pp. 2041–2043, 1998.

[21] R. P. Cowburn, "Property variation with shape in magnetic nanoelements," *J. Phys. D*, vol. 33, pp. R1–R16, 2000.

[22] W. Rave, "Magnetic ground state of a thin-film element," *IEEE Trans. Magn.*, vol. 36, no. 6, pp. 3886–3899, Nov. 2000.

Manuscript received March 2, 2005; revised May 2, 2005.